

HYDROGENATION OF GRAPHENE ON Ir(111) BY  
VIBRATIONALLY EXCITED MOLECULES



Anders Christian Løchte Jørgensen  
iNano, Aarhus University

Supervisor:  
Liv Hornekær

Department of Physics and Astronomy, Aarhus University

June 2016

## **Abstract**



# Contents

<b>1</b>	<b>Introduction</b>	<b>1</b>
<b>2</b>	<b>Graphene</b>	<b>3</b>
2.1	Graphene . . . . .	3
2.2	Graphene on Ir . . . . .	3
2.3	Hydrogenation of graphene using atomic deuterium . . . . .	3
2.4	Hydrogenation of graphene using vibrationally excited deuterium . . . . .	5
<b>3</b>	<b>Techniques</b>	<b>7</b>
3.1	Scanning Tunneling Microscopy - STM . . . . .	7
3.2	Temperature Programmed Desorption - TPD . . . . .	7
3.3	Low Energy Electron Diffraction - LEED . . . . .	7
<b>4</b>	<b>Experimental Approach</b>	<b>9</b>
4.1	The Coal Chamber . . . . .	9
4.2	STM imaging and D <sub>2</sub> dosage . . . . .	9
4.3	TPD . . . . .	9
<b>5</b>	<b>Results</b>	<b>13</b>
5.1	Graphene on Ir(111) . . . . .	13
5.2	D <sub>2</sub> on graphene . . . . .	14
5.2.1	Full hydrogen coverage . . . . .	14
5.2.2	1745°C dose . . . . .	15
5.2.3	1593°C dose . . . . .	16
5.2.4	1343°C dose . . . . .	17
5.3	TPD measurements . . . . .	18
5.3.1	Atomic and molecular D <sub>2</sub> . . . . .	18
5.4	Graphene bilayered sample . . . . .	19
5.4.1	TPD of bilayered sample . . . . .	20
5.4.2	STM images of bilayers . . . . .	20
5.4.3	LEED of bilayered sample . . . . .	22
<b>6</b>	<b>Conclusion and future perspectives</b>	<b>25</b>

6.1 conclusion and future perspectives . . . . .	25
<b>A Additional figures</b>	<b>27</b>
<b>Bibliography</b>	<b>29</b>

1

# Introduction

super trooper



# 2

## Graphene

### 2.1 Graphene

Graphene is a two dimensional honeycomb lattice of carbon atoms. Each carbon atom is  $sp^2$  hybridized where one  $s$  orbital and two  $p$  orbitals form three planar bonds with a separation angle of  $120^\circ$ . The distance between the individual carbon atoms is  $1.42 \text{ \AA}$ . Due to the flexibility of the  $sp^2$  bonds in the  $z$  direction, many other structures can be formed by a sheet of graphene, such as fullerenes, carbon nanotubes, and graphite. The graphene unit cell consists of only two lattice points, and the lattice vectors can be written as the following:

$$a_1 = \frac{a}{2}(3, -\sqrt{3}) \quad a_2 = \frac{a}{2}(3, \sqrt{3})$$

### 2.2 Graphene on Ir

As a monolayer of graphene is synthesized on top of a metal surface the underlying metal and the graphene monolayer rarely has identical lattice parameters. This causes a mismatch between the two layers and these will be rotated at an angle compared to each other. A moiré superstructure appears when this surface is examined by STM, because certain areas has carbon directly above iridium, and certain areas has carbon and iridium perfectly out of phase. Below, figure 2.1 shows the the graphene-iridium moiré unit cell.

### 2.3 Hydrogenation of graphene using atomic deuterium

The properties of graphene changes drastically with chemical functionalization of different species. The adsorption of any species is highly determined by the underlying surface, which in this study is Ir(111). The adsorption of hydrogen to the Gr/Ir surface is a highly wanted mechanism to

### 2.3. Hydrogenation of graphene using atomic deuterium

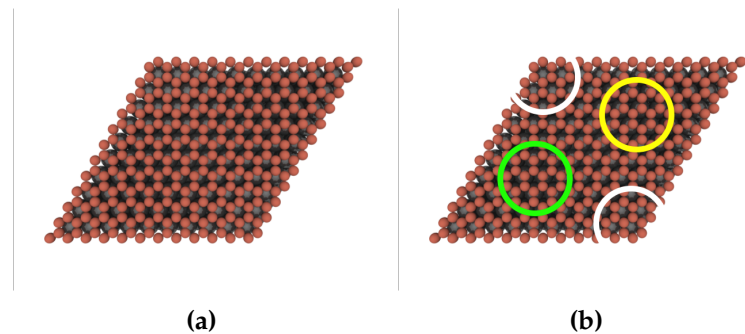


**Figure 2.1:** Graphical interpretation of the Gr/Ir moire unit cell. [1]

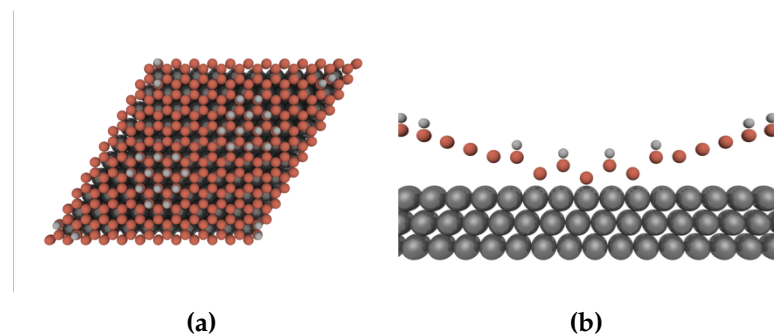


**Figure 2.2:** Graphical interpretation of the

understand, due to the special abilities arising from the functionalization of graphene by hydrogen. These effects include a bandgap opening of at least 450meV. [2] The bandgap opens up for a large number of possibilities for the usage of functionalized graphene, where the most appealing is constructing a new type of field effect transistors. Other forms of applications of functionalized graphene is within energy storage. Due to the one atom thick monolayer it is desirable to use graphene to store hydrogen, in order to increase the hydrogen storage density.

As hydrogen is adsorbed to the graphene monolayer, the structural arrangement is changed. Due to the adsorbed hydrogen atom, the graphene undergoes a transition from  $sp^2$  hybridization to  $sp^3$  hybridization. This implies that the otherwise flat graphene sheet is twisted with the angles between the bonds in the  $sp^3$  hybridization. Since every second carbon atom is turning downwards, the carbon atom constructs a bond to the underlying Ir(111) surface. This is only possible in the HCP and FCC sites of the moiré unit cell where every second carbon atom of the graphene is directly above an Iridium atom. This induces that the hydrogenation of graphene follows the moiré pattern. [3] It is therefore expected to observe a superstructure from the hydrogenated surface with the same periodicity as the moiré pattern.

A graphical interpretation of the hydrogenation of graphene on Ir(111) is shown in figure 2.2, which is made by Line Kyhl. Here it is seen that clusters of hydrogen bind to the carbon atoms in the FCC and HCP sites. Figure 2.2b demonstrates how every other carbon atom binds to the Ir(111) surface and every other binds to a hydrogen atom. Furthermore dimers of hydrogen is seen bind to the surface at the ATOP sites.

## 2.4 Hydrogenation of graphene using vibrationally excited deuterium



# 3

## Techniques

### 3.1 Scanning Tunneling Microscopy - STM

The main technique used in this study is STM, and more specifically the Aarhus STM. The working principle of the STM is the tunneling transmittivity which depends exponentially on the distance between a sharp tip and the sample. A bias is applied between the sample and the tip, and at relatively large distances the barrier that the electrons perceive is too high, and no tunneling occurs. As the distance between the sample and the tip is reduced the probability of an electron tunneling through the vacuum barrier increases until a point where tunneling happens, and the current can be measured. The tunneling current is reduced by about a factor of 10 for every ångstrøm. [4] This ensures that the STM is a very precise technique and hence essential for surface scientists. In order to achieve the tunneling current it is necessary that the tip as well as the sample is conducting. In order to create an image, the surface of the sample is scanned with the tip, which is moved by piezo-elements. The tunneling current is dependant on distance between tip and sample as well as the local density of states (LDOS). A map of the LDOS is therefore obtained when the tip is scanned across the surface of the sample. This is used to indirectly create an image of the surface.

### 3.2 Temperature Programmed Desorption - TPD

### 3.3 Low Energy Electron Diffraction - LEED



# 4

## Experimental Approach

### 4.1 The Coal Chamber

The experiments are carried out under UHV (ultra high vacuum) conditions. This is crucial because contaminants easily can adsorb to the surface which ruins the quality of the gathered data. During this project the vacuum chamber named 'The Coal Chamber' is used which is one of many vacuum chambers in the SDL lab.

The equipment mounted on The Coal Chamber, which is used in this study, is described in the following section along with the experimental approach. The sample is introduced to the coal chamber from a loadlock where the sample is attached to a transfer arm. Transfer of the sample from the loadlock to the main chamber takes place as the pressure in the loadlock is reduced sufficiently by a turbo pump. In the main chamber a manipulator is apparent in the center from where the sample can be transferred to the STM by a wobble stick. A filament lies behind the sample in the manipulator, which is used during anneals.

### 4.2 STM imaging and D<sub>2</sub> dosage

The STM was used to get a visualization of the coverage of hydrogen on the sample surface, and to analyse the sample between the different experiments.

write things about linescans, calibration and FFT/noise removal.

### 4.3 TPD

A mass spec is connected to the UHV chamber, and this was used to investigate the desorption of deuterium from the sample surface. The sample was positioned in the manipulator as the experiments were carried out. From here the nozzle of the mass spec was brought within millimeters of the sample. The temperature was logged together with the amount of deuterium detected by the

### 4.3. TPD

---

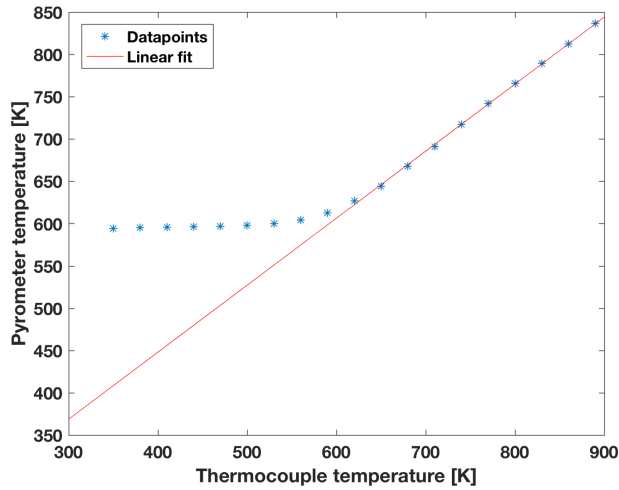


**Figure 4.1:** Calibration of the temperature during the TPD measurements. The temperature of the surface measured by an optical pyrometer is plotted against the thermocouple temperature.

mass spec. The mass spec was set to count masses of 4 amu, in order to exclude other molecules than deuterium. This setup was made with the computer program 'MASsoft' by Hiden Analytical. A Eurotherm 2704 controller was used to control the current going to the filament in the manipulator, in order to manage the temperature of the sample. The controller was programmed to ramp the sample temperature from 300K to 900K at a rate of 1K per second. At maximum temperature the eurotherm was set to rest for 30s, and then slowly decrease the temperature to a final temperature of 300K. This cycle was performed each time a TPD measurement was carried out. During this procedure most of the deuterium on the surface should be desorbed from the sample.

$$T_{surface} = T_{TC} * 0.7921 + 131.2$$

In figure 4.2a the data obtained from a typical TPD measurement is shown. Since the desorption of D<sub>2</sub> from the surface is investigated, a mass of 4 amu is monitored along with the temperature. It is seen that the temperature follows has a linear ramp except for the extremities of the temperature interval where some fluctuations start to happen. A different sample of Gr/Ir was used later on in the project, where the thermocouple seemed to have a loose connection. The temperature reading from this thermocouple dropped out at some points, and seemed unstable. Since the thermocouple was changed, and a new sample holder was used, the Eurotherm controller parameters needed to be autotuned, in order to achieve a linear temperature ramp once again. This caused some problems however, and the results from one of the TPD measurements from this sample can be seen in figure 4.3. It is seen on figure 4.3a that the temperature ramp is obviously not linear. The jumps in temperature do not seem to be systematic, which might indicate that the thermocouple as well as the controller parameters both had influence on the bad temperature ramp. The influence of the non linear ramp is also seen on the D<sub>2</sub> counts, where small peaks appear when the temperature changes rapidly. As seen on figure 4.3b another peak appears right after the initial due to the jump

in temperature. The initial peak was judged to reflect the desorption of hydrogen best, and hence this peak was used, as seen from the green circle.

Since the temperature is controlled and logged with the Eurotherm controller, it is possible to plot the counts of D<sub>2</sub> against the temperature. These plots are presented in chapter 5.

A triple gaussian function was fitted to the datapoints around the peak, in order to determine the temperature belonging to the peak. The peak value was estimated by visual observation, and the datapoints within  $\pm 60^\circ\text{C}$  are included in the fit. The temperature at the maximum of the fit was determined, and these values are presented in chapter 5 as the peak temperatures. An example of the fit to the peak values is shown in figure 4.2b. From this figure it is seen that the temperature at which the maximum counts is observed, not necessarily corresponds to the correct peak temperature. The green circle in figure 4.2b shows the found peak from which the temperature was gathered.

In order to compare the individual peaks, the background was subtracted from every datapoint. The sample was positioned stationary in front of the nozzle for a period of time before the measurements were carried out. These datapoints were used to calculate a mean background count, which was subtracted.

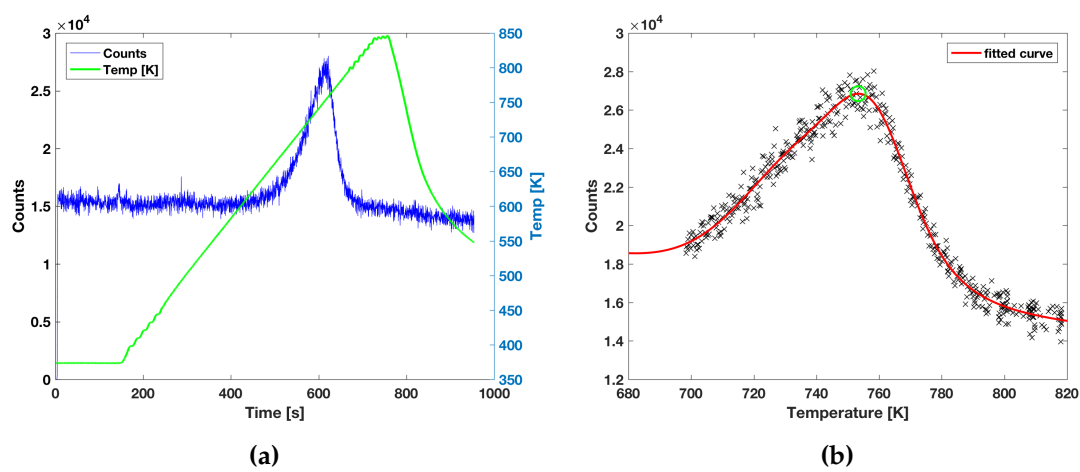


**Figure 4.2**

#### 4.3. TPD

---

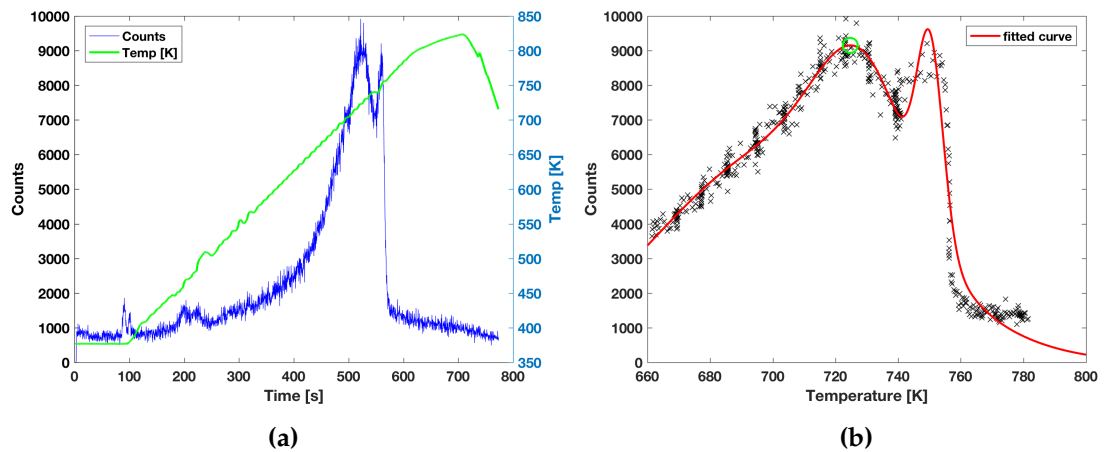


**Figure 4.3**

# 5

# Results

## 5.1 Graphene on Ir(111)

The quality of the graphene was checked before each dose of D<sub>2</sub>, in order to ensure that the amount of defects was at a minimum. STM images of pure graphene on Ir(111) are shown in this section. On figure 5.1 images of graphene on Ir(111) in different sizes are shown. Figure 5.1a shows a large image of a graphene monolayer covering the Ir(111) surface. Although the quality of the image is low, the moire pattern can be perceived as a pattern of small hexagonal structures, as outlined in the top left of the image. Also several step edges from the underlying Ir surface is seen. Several line scans has been performed on these edges, which show that the height difference is 2Å ±0.4Å. This value is consistent with the value of 0.22nm found in the literature. [5]

On figure 5.1b a high resolution image of Gr/Ir(111) is seen. The moire pattern is very prominent in this figure, which once again is outlined as the blue hexagon. and the spacing between the individual sites in the moire unit cell can be determined from a line scan. A line scan was drawn on figure 5.1b and two points were positioned in the corners of the moire unit cell in order to obtain the moire periodicity. The moiré periodicity is  $25.2 \pm 0.4\text{\AA}$  according to the literature. [6] This agrees with the measured length of  $25.24 \pm 1\text{ \AA}$  from the line scan, which is seen on figure 5.1d. Typical defects of the graphene monolayer is seen as well in this figure, as seen within the blue circle. A close look at figure 5.1b indicates that another periodic structure than the moiré pattern is present. This pattern is however more clear in figure 5.1c. This image is a zoom in of the image shown in figure 5.1b corresponding to the dashed square. The smaller pattern mentioned before is much more visible on this image. The hexagonal pattern is the graphene monolayer on top of the iridium. The graphene hexagon is sketched as the blue hexagon and the moiré pattern as seen on the two preceding figures is sketched as the dashed blue hexagon. The moiré unit cell is shown as well as the blue rhombus, where the four dark corners corresponds to the ATOP sites. The HCP and FCC sites lies at the corners of the dashed blue hexagon within the outlined moiré unit cell.

## 5.2. D<sub>2</sub> on graphene

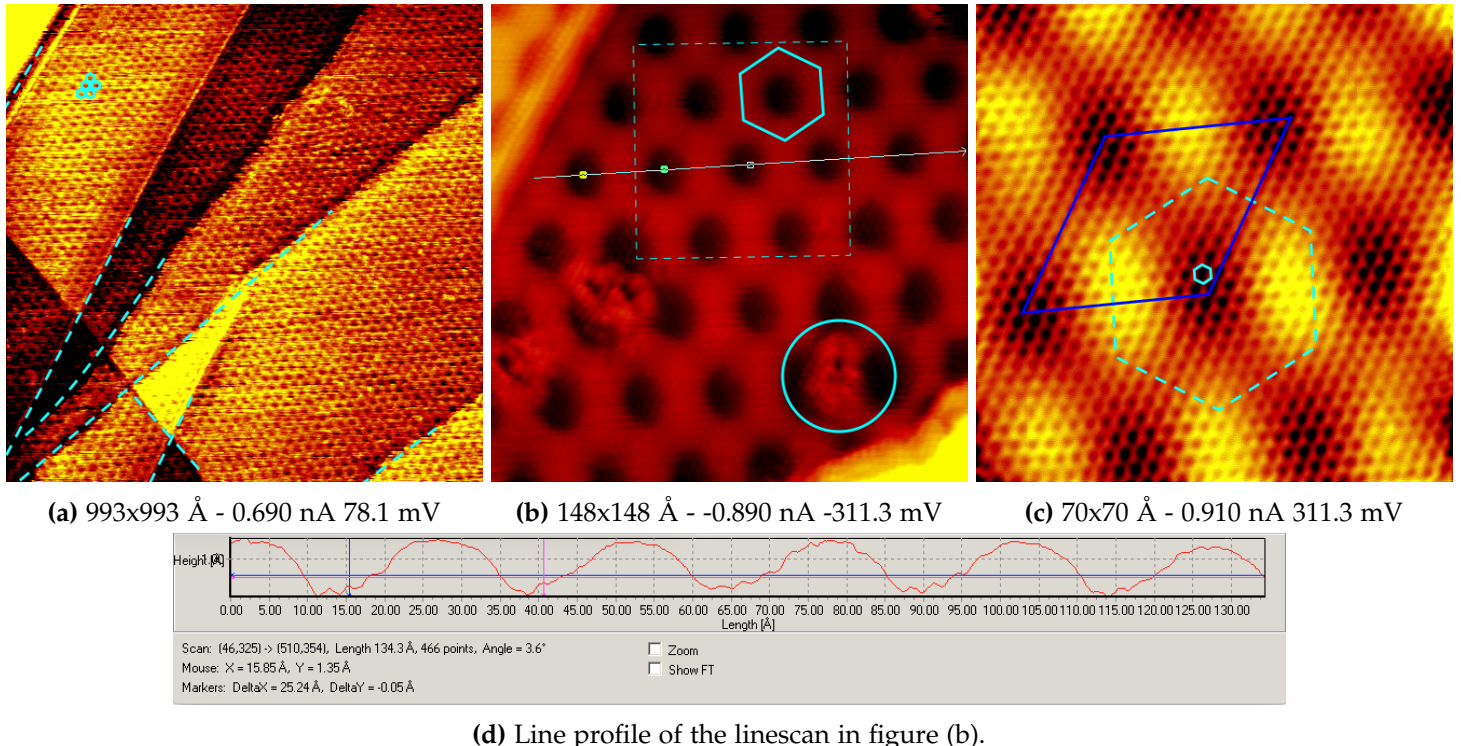


**Figure 5.1:** Clean graphene on Ir(111). (c) is a zoom in of (b) which is shown as the dashed square.

## 5.2 D<sub>2</sub> on graphene

In the following sections, the data from the dose of vibrationally excited molecules are presented. It was desirable to determine the threshold temperature of the hydrogenation of graphene. Hence the temperature of the doser was varied in order alter the flux of atoms from the doser, and thereby changing the number of hydrogen recombinations on the walls within the chamber. Therefore the data includes dosages at temperatures of, 1343°C, 1543°C and 1745°C. A dose at 1300°C were performed as well, however the STM broke, and no pictures are therefore included.

### 5.2.1 Full hydrogen coverage

STM images were made from a fully hydrogenated surface in order to compare these to the images from the short dosages. The fully hydrogenated surface was made by filling the chamber with hydrogen at a pressure of  $1 \cdot 10^{-5}$  mbar and with the iongauge set to 1.0mA. These conditions were left for 12 hours and the sample was scanned afterwards. On figure 5.2 images on different scales can be seen. As seen on figure 5.2a the sample is not just locally hydrogenated. Ring structures are seen covering the surface on this image, instead of the moiré pattern observed on figure 5.1a. These structures are however more clear on the following figure 5.2b, which is a zoom in of figure 5.2a. The most common pattern, of the hydrogenated surface, is ring shaped as structures with a bright rim and a darker center. By comparing figure 5.2b with figure 5.1b it is obvious that the adsorption of hydrogen on the surface changes the LDOS. It is noticeable

that the defects on figure 5.1b looks like the ring shaped structures seen on figure 5.2, and hence these defect might be caused by adsorbed hydrogen. Furthermore some H-structures on the saturated surface seem to melt together in a bigger structure, seen as the bone- and three point star shaped structures as pointed out in figure 5.2b. A line scan was performed on the sample in order to check the periodicity of the pattern on the hydrogenated surface. The line scan is seen on figure 5.2c and the related profile is shown in figure 5.2d. The distance between the two points is measured to  $24.2 \pm 1 \text{ \AA}$ . This value is very close to the expected periodicity of the moiré unit cell. [5]

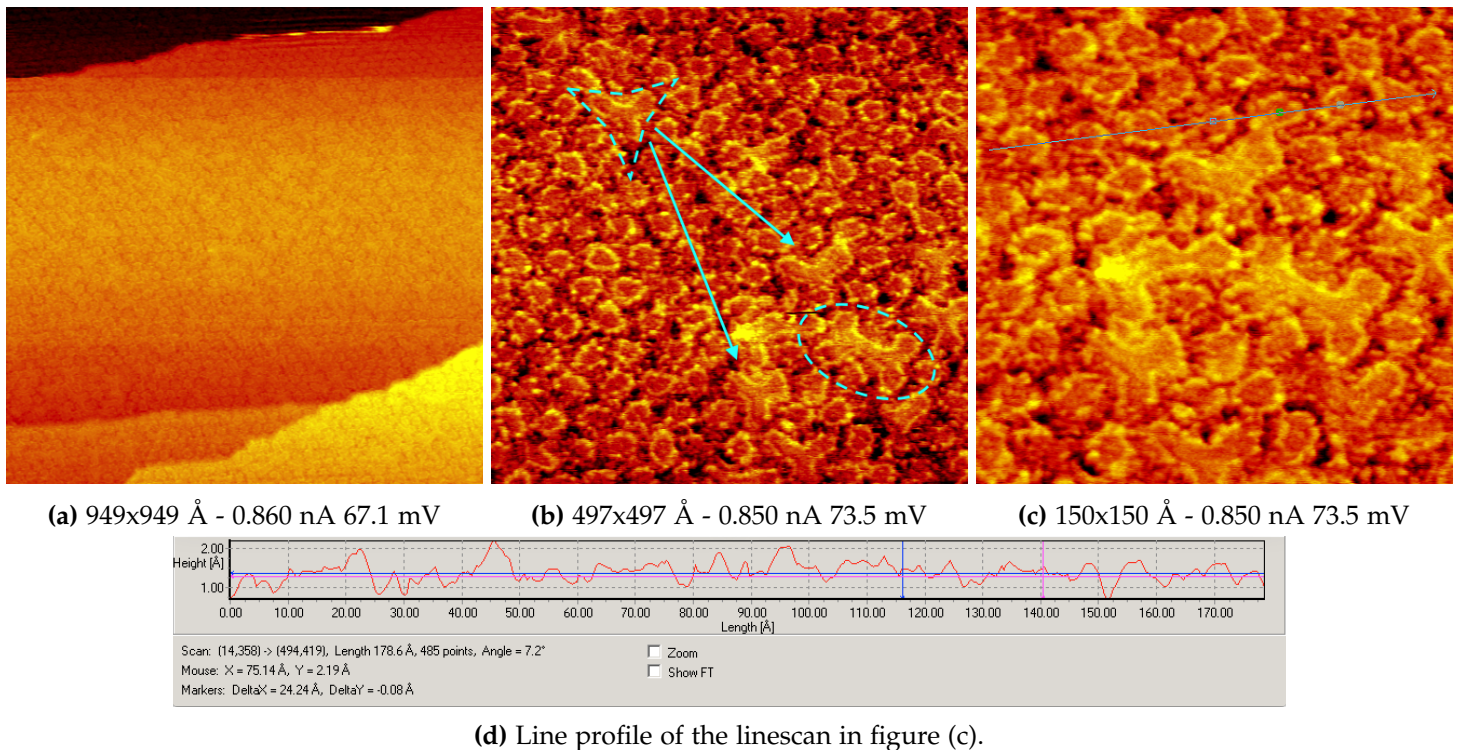


**Figure 5.2:** Fully hydrogenated Gr/Ir(111) surface after 12h D<sub>2</sub> dosage. (c) is a zoom in on (b)

### 5.2.2 1745°C dose

This dose was performed at a pirani pressure of  $6.8 \cdot 10^{-2} \text{ mbar}$ , and with the doser at a temperature of 1745°C. The dosage time was 20 min. The graphene was checked before the dose in order to ensure that no abnormal amount of defects was present. Three images at different scales are shown in figure 5.3. These pictures were taken right after the dose had ended, and the pressure dropped sufficiently. As seen on figure 5.3a, the surface is far from saturated, compared to figure 5.2a, since the moiré pattern is seen in between areas where the distinct ring structure of the hydrogenation is seen. It is also worth noting that none of the hydrogenated sites melt together to form bigger structures, which indicates that this phenomenon happens as the surface becomes saturated. In figure 5.3 each moiré unit cell has been sketched out with blue dashed lines. From this it is obvious that hydrogenation only happens at one site in the bottom left corner of the moiré unit cell. Earlier studies suggest that this is the FCC site in the moiré unit cell. [7] It is, however, seen

## 5.2. D<sub>2</sub> on graphene

that the hydrogenation expands to the HCP site as well in some of the unit cells, as shown with the dark blue circle.

Individual hydrogen atoms are not distinguishable from the STM images, and therefore the coverage is estimated as a percentage of the number of hydrogenated unit cells to the total number of unit cells. Figures 5.3b and 5.3c were used to calculate an estimate of the hydrogenation of the surface. The coverage on figure 5.3b was calculated to 41% and the coverage on figure 5.3c was calculated to 29%. This means that about one third of the unit cells is hydrogenated after a dosage of excited molecules for 20 min, at a chamber pressure of  $5 \cdot 10^{-5}$  mbar.

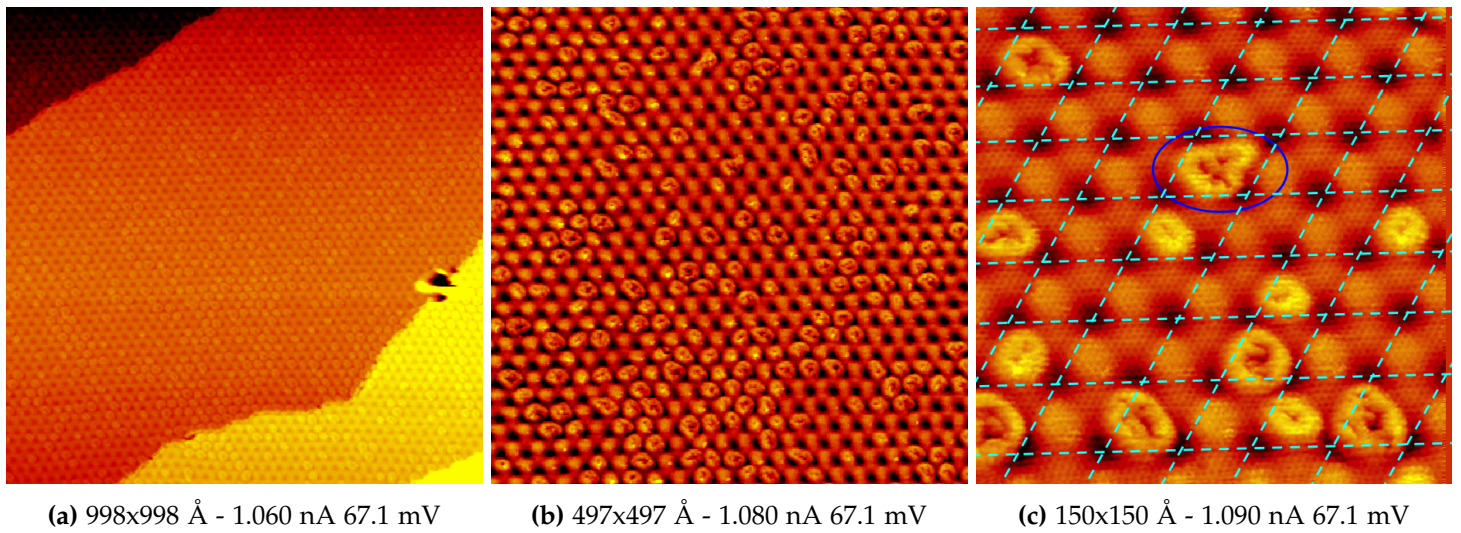


**Figure 5.3:** Hydrogenated Gr/Ir surface after dose of D<sub>2</sub> at a doser temperature of 1745°C.

### 5.2.3 1593°C dose

This dose was performed at a pirani pressure of  $6.8 \cdot 10^{-2}$  mbar and a doser temperature of 1593°C. Again the dose had a duration of 20 min. The images obtained after the dose are shown in figure 5.4. The resemblance between the pictures shown in figure 5.3 and 5.4 is quite high. Again the ring shaped structures are seen, and the shape of these are very similar to the ones observed earlier. Figures 5.4a and 5.4b were used to calculate the coverage of hydrogenation, with values of 32% and 25% respectively. These values are however very position dependant, and therefore they do not necessarily reflect the accurate coverage. It is however clear that hydrogenation of the surface has occurred.

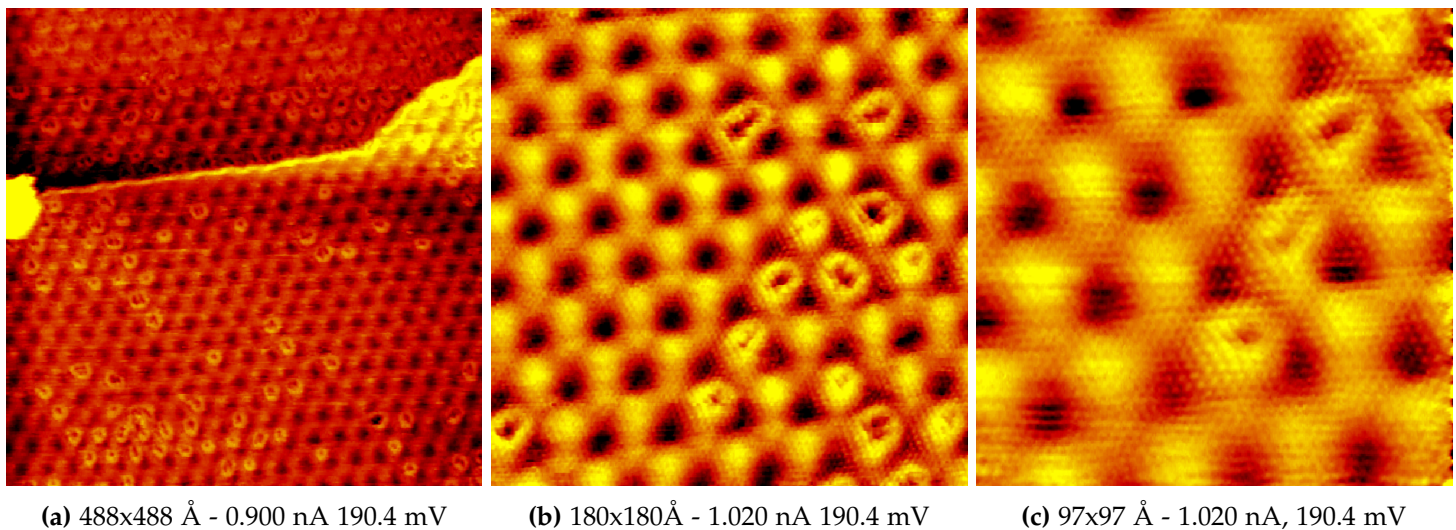


**Figure 5.4:** Hydrogenated Gr/Ir surface after dose of D<sub>2</sub> at a doser temperature of 1593°C.

#### 5.2.4 1343°C dose

The pirani pressure was measured to  $6.8 \cdot 10^{-2}$  mbar, and the doser had a temperature of 1343°C during this dose. Hydrogen was dosed for 20 min as earlier. As seen on figure 5.5 several high quality pictures of the sample was taken. On figure 5.5a it would seem like some hydrogen is adsorbed due to the observation of several ring shaped structures. As a smaller image is taken such as the one in figure 5.5b the defects looks somewhat different from those seen earlier on figures 5.4b and 5.3c. The ring shaped structures are much smaller in diameter on figure 5.5b, even though the scanning parameters are close to each other.

A high resolution image is seen on figure 5.5c, where the hexagonal graphene is highly visible. On this picture it is clear that the graphene is defected, although it is unclear whether this is due to the presence of hydrogen. It is also seen that the shape of the sites in the moiré unit cell looks different than earlier although both pictures are from the same scan session. This is due to a tip effect, where the LDOS of the tip probably has changed, which has an influence on the tunnelling current. This might happen if the tip picks up an atom from the surface, or if the physical dimensions of the tip changes after a tip treatment.

It should be noted that the graphene had defects before the dose was initiated. The abundance of these defects was indistinguishable, when comparing before and after the dose. Therefore it is not possible to conclude whether the threshold temperature of the hydrogen adsorption from excited molecules lies at 1340°C. It is however very likely that no hydrogen is adsorbed. In order to investigate the threshold temperature further, it would be rational to conduct TPD measurements of the sample after hydrogen dosage at 1343 °C.

### 5.3. TPD measurements

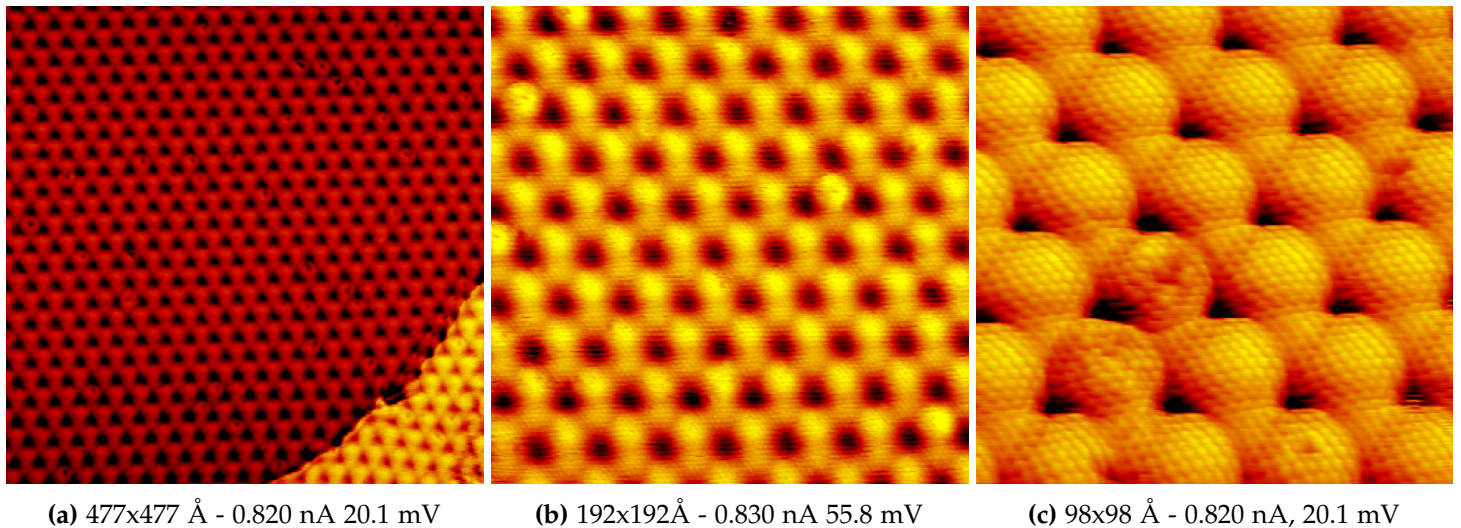


**Figure 5.5:** Hydrogenated Gr/Ir surface after dose of D<sub>2</sub> at a doser temperature of 1340°C.

## 5.3 TPD measurements

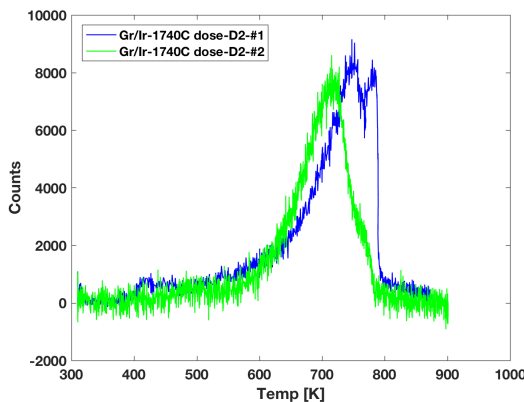
In the following sections, TPD measurements from graphene on Ir(111) exposed to both hot molecules and atoms are compared. These data were gathered twice from two different samples as explained in chapter 4. Furthermore the effect of a bilayered sample on the hydrogenation of graphene was investigated by conducting TPD measurements.

### 5.3.1 Atomic and molecular D<sub>2</sub>

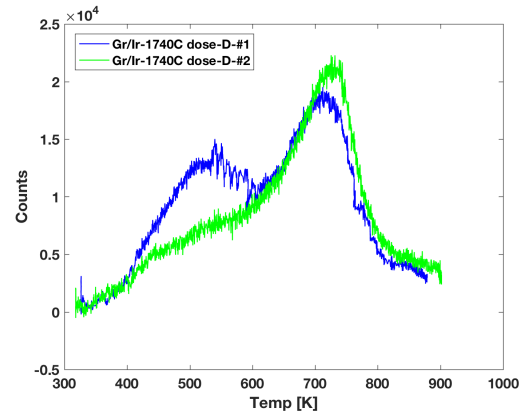
In figure 5.6 below, the data from the TPD is gathered in two different figures. TPD measurements were made following doses of both vibrationally excited molecules and atoms. Figure 5.6a shows the TPD data following a 60 min dose of D<sub>2</sub> at a chamber pressure of  $5 \cdot 10^{-7}$  mbar and a doser temperature of 1740°C. Figure 5.6b shows the data following a 60 min dose of hydrogen atoms at a chamber pressure of  $5 \cdot 10^{-7}$  mbar and a doser temperature of 1740°C.

After dosage of excited molecules a single peak is observed. On figure 5.6a this peak is seen from two datasets matching the two different samples. It is worth noting that the peaks are shifted compared to each other. The reason for this might be the fact that the sample temperature was measured using two different thermocouples as explained in chapter 4. For the second dataset, corresponding to the blue graph, a quite big peak is seen after the main peak, at a temperature of about 800K. This is due to a temperature spike caused by the Eurotherm temperature controller. The calibration of the Eurotherm during this experiment was poor, which results in noticeable fluctuations in the desorption of hydrogen. This phenomenon is also observed on figure 5.6b, on the blue graph. This dataset was gathered during the same chamber and sample conditions as the blue graph in figure 5.6a. Therefore the calibration of the Eurotherm was poor as well, which is seen after the small peak at about 500K in figure 5.6b. Here several small bumps are seen due to the non-linear temperature ramp.

Sample	fig.5.6a blue	fig.5.6a green	fig.5.6b blue	fig.5.6b green	fig.5.7 green	fig.5.7 red	mean
Peak T [K]	724.8	698.4	694.0	709.1	739.1	753.4	719.8



(a) TPD of Gr/Ir after 1 hour dose of D<sub>2</sub> with a doser temperature of 1740 °C.



(b) TPD of Gr/Ir after 1 hour dose of atomic hydrogen with a doser temperature of 1740 °C.

**Figure 5.6:** TPD measurements following doses of D<sub>2</sub> and hot atoms. (a) shows two graphs following from D<sub>2</sub> doses and (b) shows two graphs following from doses with hot atoms

The temperature at the peak was found by the procedure described in chapter 4. The single peak in figure 5.6a must correspond to the hydrogen adsorbed on the HCP and FCC sites in the moiré unit cell. This statement is supported by the preceding STM pictures that show no sign of hydrogen dimers in the ATOP sites. The temperature of this peak was found for 6 datasets in all, and the values of these are shown in the table below, along with the mean value.

Another peak appears when observing the Gr/Ir sample after it has been dosed with hot atoms as seen on figure 5.6b. The green graph was initially observed, and from this it is obvious that more hydrogen desorbs from the surface at lower temperature, compared to the green graph on figure 5.6a. After a second try however, an actual peak was observed. The temperature of this peak was found by the same procedures as earlier, and the value was found to be 550.4K. This suggests that a different type of Gr-H bond is present. The most plausible explanation is the presence of hydrogen dimers on the ATOP site of the moiré unit cell. The fact that no hydrogen adsorbs as dimers, when excited molecules are dosed, is supported heavily by the fact that this peak around 550K is completely absent from all the data obtained from the molecular dosage seen in figures 5.6a and 5.7.

## 5.4 Graphene bilayered sample

As a further study of the adsorption of hydrogen on Gr/Ir, patches of graphene bilayers were grown on the sample by annealing in ethylene for a long period of time. The sample was investigated with several techniques, and the results are presented in the following sections.

## 5.4. Graphene bilayered sample

### 5.4.1 TPD of bilayered sample

TPD measurements were conducted on the sample before and after the long anneal. The red graph in figure 5.7 is the results following a 60 min dose of D<sub>2</sub> at a chamber pressure of  $1.04 \cdot 10^{-6}$ mbar and with a doser temperature of 1740°C. The number of D<sub>2</sub> counts at the peak is roughly 13.000, which is a lot higher than the peaks in figure 5.6a with peak values around 8.000-9.000. This indicates that the surface was not saturated during the previous TPD measurements. Besides the higher peak value, the graph looks similar to the previous data, with a single peak around 700K. The green graph corresponds to the sample after bilayers supposedly were grown. Bilayers were grown by exposing the sample to ethylene at a pressure of  $1 \cdot 10^{-6}$ mbar for 60 min, while the sample was heated to 990°C. The sample was dosed with atomic hydrogen at a chamber pressure of  $1.04 \cdot 10^{-6}$ mbar and with a doser temperature of 1740K as well as before. It is seen that the peak value this time is around 6.000, which means that the increased amount of bilayers reduce the amount of hydrogen on the surface by a significant amount. This suggests that hydrogen is not adsorbed on the bilayered graphene. This theory is supported by the STM pictures below. It should be noted that only two datasets were gathered from this experiment. The peak intensity from the TPD measurements tends to vary slightly and hence the amount of bilayers grown on the sample might not be perfectly related to the drop in peak intensity.

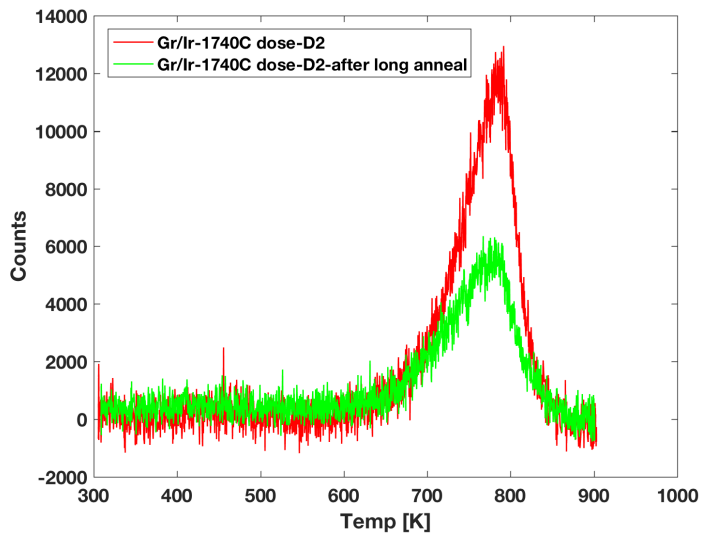


**Figure 5.7:** TPD measurements after doses of D<sub>2</sub> at a pressure of  $1.04 \cdot 10^{-6}$  and a doser T of 1740°C. The red graph is prior to a 60 min growth of bilayers where the 990°C hot sample was exposed to ethylene for 60 min at a pressure of  $1 \cdot 10^{-6}$ mbar

### 5.4.2 STM images of bilayers

In the following section STM images of bilayer patches are included. These images are made prior to the long anneal, and are therefore not directly related to the experiment mentioned in the preceding section. It was not possible to make images of the sample after the long anneal in ethylene, since the STM was broken. Bilayers were however present on the surface prior to the

long anneal, and the following images show some of the key points about these.

The images in figure ?? are made after the 12 hour dose of hydrogen at a chamber pressure of  $1 \cdot 10^{-5}$  mbar with the ion gauge turned on. Hence the surface is fully hydrogenated which is somehow different to see due to the large images. On figure 5.8a, the three-point-star-structures characteristic for the hydrogenated surface are however seen, which is pointed out with the blue arrows. Bilayer patches are seen on the top half of the figure, and none of the structures characteristic for the fully hydrogenated surface are seen. A new superstructure is however seen with the individual flower-like structures, with a center circle surrounded by six other circles, construct a bigger pattern.

On figure 5.8b a linescan was made across the edge of the graphene monolayer-bilayer edge. The corresponding line profile is shown in figure 5.8d, and from this the height difference is measured to  $2.97 \pm 0.5$  Å. The bilayer edge is therefore significantly higher than the Iridium step edge, and much closer to the layer height of HOPG which is 0.35nm. [8]

In order to investigate the bilayer superstructure further, a zoom in of figure 5.8b was made as seen in figure 5.8c. The graphene sheet is seen due to the atomic resolution, and it is obvious that no hydrogen is adsorbed to the surface. This is consistent with the data from the TPD measurements. Furthermore it is seen that the consistency in the superstructure is absent. Some areas of the bilayer has a cluster of three circles forming a triangle that points either up or down. These are highlighted in the left side of the picture. Other areas seem to have the flower-like structure mentioned earlier, but with an overlapping hexagon. An attempt to determine the periodicity of the superstructure was done by doing a linescan between two identical parts of the pattern. As seen on figure 5.8c the linescan was drawn between two down facing triangles, and the distance between these were measured from the bottom corner. The line profile is shown in figure 5.8e and the length between the points is measured to  $45.78 \pm 1$  Å.

## 5.4. Graphene bilayered sample

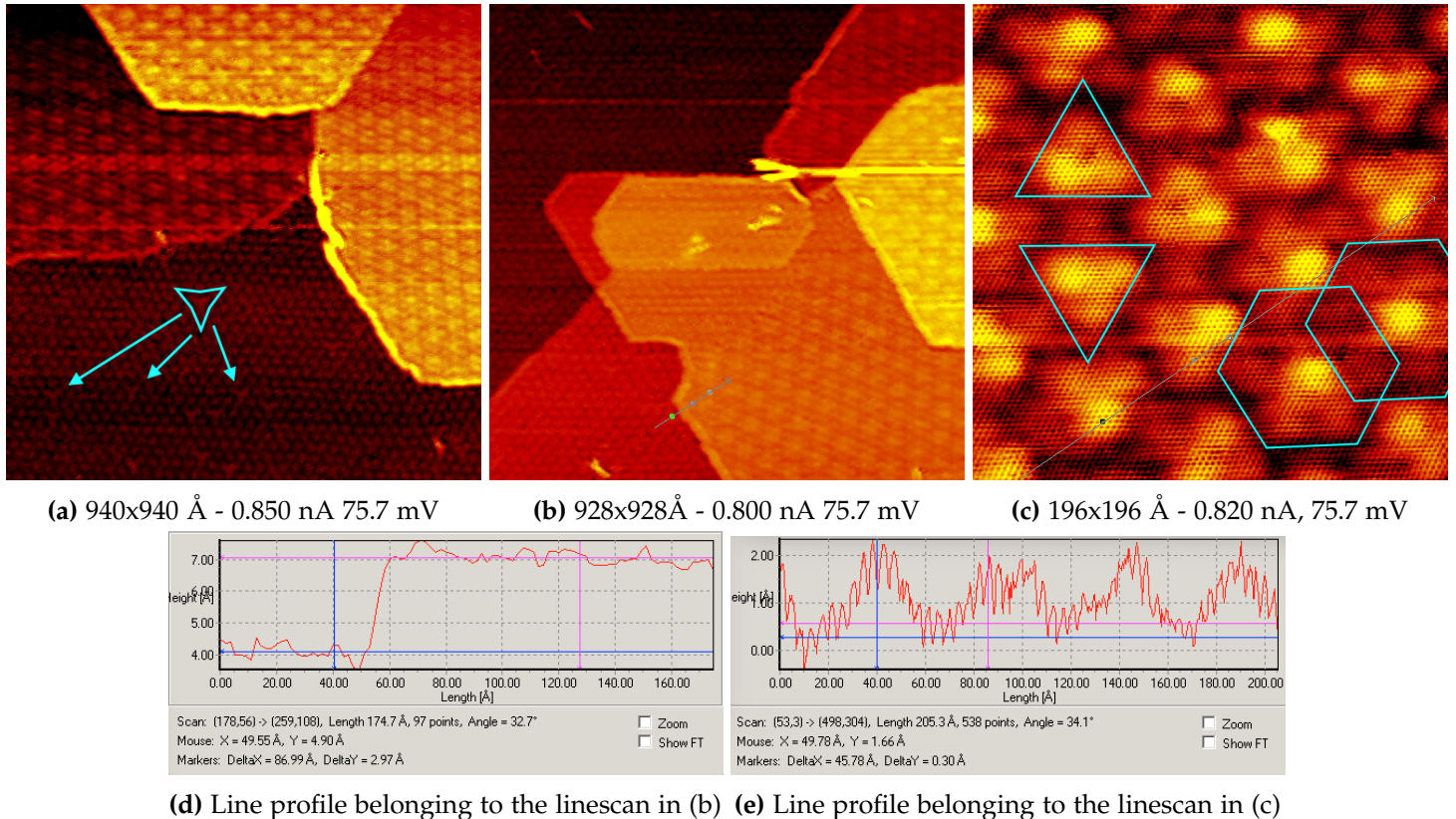


**Figure 5.8:** Patches of bilayered graphene on Ir after a hydrogen dose at  $1 \cdot 10^{-5}$ mbar for 12h.

### 5.4.3 LEED of bilayered sample

LEED was performed on the sample after an ethylene anneal with a chamber pressure of  $7 \cdot 10^{-7}$ mbar. The figures in 5.9 show pictures of the fluorescent screen within the UHV chamber from which the LEED was performed. The image on figure 5.9a shows the fluorescent screen after the untreated sample was exposed to an electron beam with an energy of 145eV. The spots marked out with the marked arrows show the diffraction pattern from the underlying Ir(111) surface, as well as the graphene sheet on top of the surface. [6]

The sample was then flashed to a low temperature in order to maintain any bilayers, and the sample was once again exposed to an electron beam of energy 145eV. The top and bottom right corner of the hexagonal pattern is enlarged in figure 5.9b. From this figure it is clear that some extra spots appear around the Ir and C spots pointed out in the previous figure. These spots arise from the moiré pattern of the graphene on Ir(111) surface. The reason why these spots were absent in the previous figure might be caused by a high amount of contaminants on the surface. These ruin the periodicity of the surface, and hence also the electron scattering, which then becomes smeared out. After annealing to a low temperature these contaminants should be gone, leaving the surface clean with small patches of bilayered graphene. The patches of bilayered graphene should however also cause a different scattering due to the changed periodicity as seen in figure 5.8c. If figure 5.9b and 5.9c is compared it does look like the spot belonging to the carbon atoms

#### 5.4. Graphene bilayered sample

and the surrounding moiré spots in figure 5.9b are less distinct. These results might therefore indicate that bilayers are present on the surface in figure 5.9b and to a lesser extent in figure 5.9c. Since the picture in figure 5.9c is taken prior to an 1090°C anneal, it is reasonable to conclude that the bilayer patches desorb from the surface when annealing to this temperature.[Reference til desorption af bilayers?]

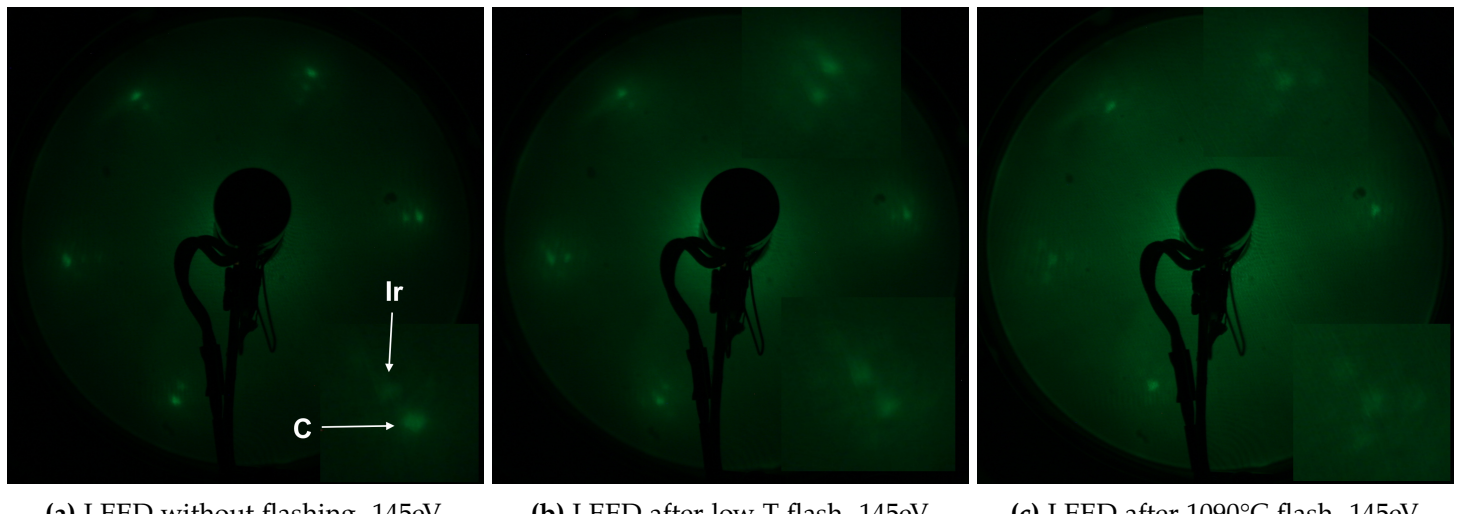


**Figure 5.9:** LEED pictures from the Gr/Ir sample with bilayers. [Reference til Antonija/Hoffman-lab]



# 6

## **Conclusion and future perspectives**

### **6.1 conclusion and future perspectives**



A

## Additional figures



# Bibliography

- [1] Line Kyhl.
- [2] Richard Balog, Bjarke Jørgensen, Louis Nilsson, Mie Andersen, Emile Rienks, Marco Bianchi, Mattia Fanetti, Erik Laegsgaard, Alessandro Baraldi, Silvano Lizzit, Zeljko Sljivancanin, Flemming Besenbacher, Bjørk Hammer, Thomas G Pedersen, Philip Hofmann, and Liv Hornekær. Bandgap opening in graphene induced by patterned hydrogen adsorption. *Nature Materials*, 9(4):315–319, 4 2010.
- [3] Line Kyhl, Richard Balog, Thierry Angot, Liv Hornekær, and Régis Bisson. Hydrogenated graphene on ir(111): A high-resolution electron energy loss spectroscopy study of the vibrational spectrum. *Phys. Rev. B*, 93:115403, Mar 2016.
- [4] Gerd Binnig and Heinrich Rohrer. Scanning tunneling microscopy—from birth to adolescence. *Rev. Mod. Phys.*, 59:615–625, Jul 1987.
- [5] Johann Coraux, Alpha T N'Diaye, Martin Engler, Carsten Busse, Dirk Wall, Niemma Buckanie, Frank-J Meyer zu Heringdorf, Raoul van Gastel, Bene Poelsema, and Thomas Michely. Growth of graphene on ir(111). *New Journal of Physics*, 11(2):023006, 2009.
- [6] Alpha T N'Diaye, Johann Coraux, Tim N Plasa, Carsten Busse, and Thomas Michely. Structure of epitaxial graphene on ir(111). *New Journal of Physics*, 10(4):043033, 2008.
- [7] Jakob Jørgensen, Antonija Grubisic Cabo, Line Kyhl Hansen, Richard Balog, Philip Hofmann, and Liv Hornekær. Unpublished.
- [8] J. Červenka and C. F. J. Flipse. Structural and electronic properties of grain boundaries in graphite: Planes of periodically distributed point defects. *Phys. Rev. B*, 79:195429, May 2009.